Physics and Chemistry of Minerals (2018) 45:745–758
https://doi.org/10.1007/s00269-018-0959-9

ORIGINAL PAPER

Siudaite, $Na_8(Mn^{2+}{}_2Na)Ca_6Fe^{3+}{}_3Zr_3NbSi_{25}O_{74}(OH)_2Cl{\cdot}5H_2O$: a new eudialyte-group mineral from the Khibiny alkaline massif, Kola Peninsula

Nikita V. Chukanov[1,2] · Ramiza K. Rastsvetaeva[3] · Łukasz Kruszewski[4] · Sergey M. Aksenov[3,5,8] · Vyacheslav S. Rusakov[6] · Sergey N. Britvin[7] · Svetlana A. Vozchikova[1]

Received: 2 February 2018 / Accepted: 2 March 2018 / Published online: 9 March 2018

Abstract

The new eudialyte-group mineral siudaite, ideally $Na_8(Mn^{2+}{}_2Na)Ca_6Fe^{3+}{}_3Zr_3NbSi_{25}O_{74}(OH)_2Cl{\cdot}5H_2O$, was discovered in a peralkaline pegmatite situated at the Eveslogchorr Mt., Khibiny alkaline massif, Kola Peninsula, Russia. The associated minerals are aegirine, albite, microcline, nepheline, astrophyllite, and loparite-(Ce). Siudaite forms yellow to brownish-yellow equant anhedral grains up to 1.5 cm across. Its lustre is vitreous, and the streak is white. Cleavage is none observed. The Mohs' hardness is 4½. Density measured by hydrostatic weighing is 2.96(1) g/cm^3. Density calculated using the empirical formula is equal to 2.973 g/cm^3. Siudaite is nonpleochroic, optically uniaxial, negative, with $\omega = 1.635(1)$ and $\varepsilon = 1.626(1)$ ($\lambda = 589$ nm). The IR spectrum is given. The chemical composition of siudaite is (wt%; electron microprobe, H_2O determined by HCN analysis): Na_2O 8.40, K_2O 0.62, CaO 9.81, La_2O_3 1.03, Ce_2O_3 1.62, Pr_2O_3 0.21, Nd_2O_3 0.29, MnO 6.45, Fe_2O_3 4.51. TiO_2 0.54, ZrO_2 11.67, HfO_2 0.29, Nb_2O_5 2.76, SiO_2 47.20, Cl 0.54, H_2O 3.5, –O = Cl − 0.12, total 99.32. According to Mössbauer spectroscopy data, all iron is trivalent. The empirical formula (based on 24.5 Si atoms *pfu*, in accordance with structural data) is $[Na_{7.57}(H_2O)_{1.43}]_{\Sigma 9}(Mn_{1.11}Na_{0.88}Ce_{0.31}La_{0.20}Nd_{0.05}Pr_{0.04}K_{0.41})_{\Sigma 3}(H_2O)_{1.8}(Ca_{5.46}Mn_{0.54})_{\Sigma 6}(Fe^{3+}{}_{1.76}Mn^{2+}{}_{1.19})_{\Sigma 2.95}Nb_{0.65}(Ti_{0.20}Si_{0.50})_{\Sigma 0.71}(Zr_{2.95}Hf_{0.04}Ti_{0.01})_{\Sigma 3}Si_{24.00}Cl_{0.47}O_{70}(OH)_2Cl_{0.47}{\cdot}1.82H_2O$. The crystal structure was determined using single-crystal X-ray diffraction data. The new mineral is trigonal, space group $R3m$, with $a = 14.1885(26)$ Å, $c = 29.831(7)$ Å, $V = 5200.8(23)$ Å^3 and $Z = 3$. Siudaite is chemically related to georgbarsanovite and is its analogue with Fe^{3+}-dominant $M2$ site. The strongest lines of the powder X-ray diffraction pattern [d, Å (I, %) (hkl)] are: 6.38 (60) (–114), 4.29 (55) (–225), 3.389 (47) (131), 3.191 (63) (–228). 2.963 (100) (4–15), 2.843 (99) (–444), 2.577 (49) (3–39). Siudaite is named after the Polish mineralogist and geochemist Rafał Siuda (b. 1975).

Keywords New mineral · Siudaite · Eudialyte group · Crystal structure · IR spectroscopy · Mössbauer spectroscopy · Peralkaline pegmatite · Khibiny massif

Electronic supplementary material The online version of this article (https://doi.org/10.1007/s00269-018-0959-9) contains supplementary material, which is available to authorized users.

✉ Nikita V. Chukanov
chukanov@icp.ac.ru

[1] Institute of Problems of Chemical Physics, Russian Academy of Sciences, Chernogolovka, Moscow Region 142432, Russia

[2] Faculty of Geology, Moscow State University, Vorobievy Gory, Moscow 119991, Russia

[3] FSRC "Crystallography and Photonics", Russian Academy of Sciences, Leninskii pr. 59, Moscow 119333, Russia

[4] Institute of Geological Sciences, Polish Academy of Sciences, Twarda 51/55 str. 00-818, Warsaw, Poland

[5] Nesmeyanov Institute of Organoelement Compounds, Russian Academy of Sciences, GSP-1, Vavilova St. 28, V-334, Moscow 119991, Russia

[6] Faculty of Physics, Moscow State University, Vorobievy Gory 1-2, Moscow 119991, Russia

[7] Department of Crystallography, Institute of Earth Sciences, Saint Petersburg State University, Universitetskaya Nab. 7/9, 199034 St., Petersburg, Russia

[8] Present Address: Department of Civil and Environmental Engineering and Earth Sciences, University of Notre Dame, Notre Dame, IN 46556, USA

Introduction

Eudialyte-group minerals are of scientific interest as important concentrators of rare elements (mainly, Zr and *REE*) in agpaitic alkaline rocks and a potential source of *REE*, Zr, Hf, Nb and Ta for industrial use (Lebedev 2003; Lebedev et al. 2003; Zakharov et al. 2011; Friedrich et al. 2016; Davis et al. 2017).

Members of the eudialyte group are represented by trigonal (space groups $R\bar{3}m$, $R3m$, or $R3$) microporous framework hetero polyhedral zircono- and titanosilicates which are characterized by a unique structural and chemical complexity and variability (Johnsen and Gault 1997; Johnsen and Grice 1999; Johnsen et al. 2003; Chukanov et al. 2004; Bulakh and Petrov 2004; Rastsvetaeva 2007; Schilling et al. 2011; Rastsvetaeva and Chukanov 2012; Rastsvetaeva et al. 2012). At present eudialyte group includes 28 mineral species. In accordance with the ordering of extra-framework cations, 12- and 24-layer species (with the *c* parameter of the unit-cell of ~ 30 and ~ 60 Å, respectively) are distinguished (Rastsvetaeva and Chukanov 2012). However, 24-layer minerals are very rare and are formed in minor amounts, under very specific conditions (Rastsvetaeva and Khomyakov 2003; Rastsvetaeva et al. 2015). Due to the structural features associated primarily with the selective sorption of elements from mineral-forming solutions and melts, eudialyte-group minerals are considered as indicators of magmatic and metasomatic processes (Ageeva et al. 2002; Schilling et al. 2009; Sjöqvist et al. 2013).

The simplified general formula of 12-layer eudialyte-group minerals is $[N1N2N3N4N5]_3M1_6M2_3M3M4Z_3(Si_9O_{27})_2(Si_3O_9)_2Ø_{4-6}X1X2$ where Si_9O_{27} and Si_3O_9 are nine- and three-membered rings of vertice-sharing tetrahedra, *M*1 are cations (Ca, Mn^{2+}, *REE*, Na, Sr, Fe^{2+}) that form a six-membered ring of edge-sharing $M1O_6$-octahedra; *M*2 is a group of closely spaced sites that can be statistically occupied by ${}^{IV,V}Fe^{2+}$, ${}^{V,VI}Fe^{3+}$, ${}^{IV,V,VI}Mn^{2+}$, ${}^{V,VI}Na^{+}$, ${}^{IV,V}Zr^{4+}$, ${}^{VI}Ta^{5+}$, as well as subordinate ${}^{VII}K^{+}$; *M*3 and *M*4 are tetrahedrally (Si, S) and octahedrally (Nb, Ti, W, Na) coordinated atoms that occupy groups of closely spaced sites near the centers of two kinds of 9-membered rings of SiO_4 tetrahedra; the *Z* site has octahedral coordination and can contain Zr, Ti and Nb; Ø = O, OH, H_2O; *N*1–*N*5 are extra-framework cations (Na, H_3O^+, K, Sr, *REE*, Y, Ba, Mn^{2+}, Ca) or H_2O; *X*(1) and *X*(2) are extra-framework water molecules, halide anions (Cl^-, F^-) and anionic groups (OH^-, CO_3^{2-}, SO_4^{2-}, AlO_4^{5-}, MnO_4^{6-}). The *M*1 cations can be disordered, or ordered and alternate in the octahedral ring. The sites *N*1–*N*5, Ø, *X*1, *X*2, *M*2, *M*3 and *M*4 can be partly vacant.

The *N*4 site concentrates selectively bi- and trivalent extra-framework cations (Ca^{2+}, Mn^{2+}, Sr^{2+}, REE^{3+}), whereas other *N*-sites are usually Na-, H_3O^+- or H_2O-dominant (Johnsen and Grice 1999; Rastsvetaeva et al. 2012). In particular, in georgbarsanovite $Na_{12}(Mn,Sr,REE)_3Ca_6Fe_3^{2+}Zr_3NbSi_{25}O_{76}Cl_2{\cdot}H_2O$ the *N*4 site is predominantly occupied by Mn^{2+} (Khomyakov et al. 2005).

This paper describes a new eudialyte-group mineral **siudaite**, which is the Fe^{3+}-dominant (in the *M*2 site) analogue of georgbarsanovite. Siudaite was found in a peralkaline pegmatite situated at the western slope of the Eveslogchorr Mt., Astrophyllitovyi Stream valley, Khibiny alkaline massif, Kola Peninsula, Russia. The geographical coordinates of the locality are 67° 40′ 02″N, 33° 55′ 28″E. The host rock is astrophyllite- and aenigmatite-bearing rischorrite, which is a peralkaline nepheline syenite. Siudaite is a product of hydrothermal alteration of a primary eudialyte-group mineral presumably related to georgbarsanovite. Further alteration resulted in the oxidation of Mn^{2+} to Mn^{3+} and formation of cherry-red to purple rims of so-called "oxyeudialyte" around siudaite grains, which is a typical process for Mn-rich eudialyte-group minerals from pegmatites of the Khibiny massif (Kostyleva-Labuntsova et al. 1978).

The new mineral is intimately associated with aegirine, albite, microcline, nepheline, astrophyllite, and loparite-(Ce) (Figs. 1, 2, 3). Siudaite is partly substituted by "zirfesite", an amorphous hydrous silicate of Zr and Fe^{3+}, which is a typical product of supergene alteration of eudialyte-group minerals in the Khibiny massif (Kostyleva-Labuntsova et al. 1978).

Siudaite is named after the Polish mineralogist and geochemist Rafał Siuda (b. 1975), a specialist in mineralogy and geochemistry of supergene zones of ore deposits in the Lower Silesia area in Poland. Currently, peralkaline pegmatites of the Khibiny-Lovozero complex are in the sphere of

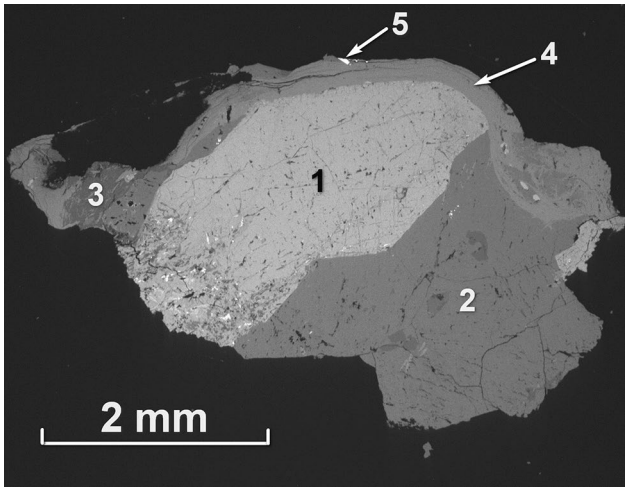

Fig. 1 Siudaite (1) in association with microcline (2), albite (3), aegirine (4) and loparite-(Ce) (5). Polished section, BSE image

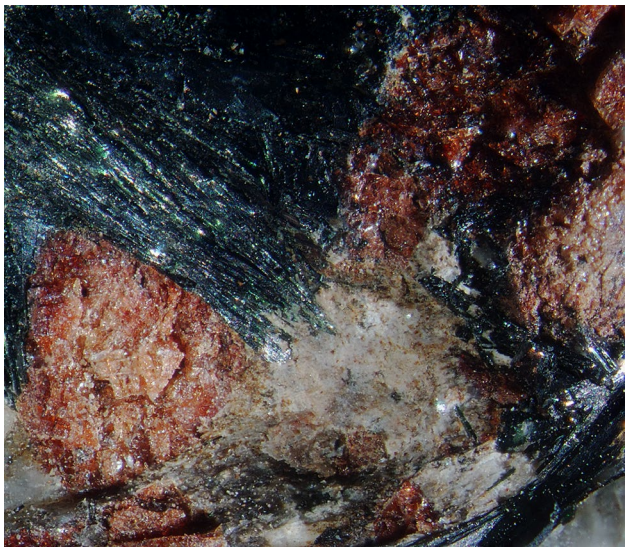

Fig. 2 Siudaite grains (orange–yellow with red rim) with aegirine (dark green) and microcline (white). Field width 8 mm

Fig. 3 Grains of oxidized siudaite (red, with relics of initial yellow phase) with aegirine (dark green in the upper part of the specimen), nepheline (greenish grains left and in centrum), microcline (white right), and astrophyllite (in the lower part of the specimen). Field width 7 cm

his scientific interest. Rafał Siuda used to be an employee of the Museum of Earth, Polish Academy of Sciences and now is employed in the Institute of Geochemistry, Mineralogy and Petrology, Faculty of Geology, University of Warsaw. He was among the organizers of the field trip during which specimens with siudaite were collected by one of us (Ł. K.) and also by Rafał Siuda himself. The trip was a part of the activity of the Young Geologists' Club of the University of Warsaw.

It should be noted that besides the type locality of siudaite, a similar material containing cherry-red grains of an eudialyte-group mineral was found as an important (rock-forming) constituent of aegirine-rich pegmatitic rocks collected by Krzysztof Dembicz above the original find place, at the left bank of the Astrofillitovyi Stream, near its northwestern bifurcation. This mineral is macroscopically and paragenetically identical to oxidized siudaite.

The mineral and its name have been approved by the IMA Commission on New Minerals, Nomenclature and Classification (IMA No. 2017-092). The type material (a part of the holotype specimen) is deposited in the Mineralogical and Petrographical Section, Collection of the Museum of Earth PAS (Muzeum Ziemi Polskiej Akademii Nauk), aleja Na Skarpie 20/26, PL-00-488, Warsaw, Poland, with the catalogue number MZI III/1/541.

Experimental methods

Five chemical analyses were carried out using an Oxford INCA Wave 700 electron microprobe (WDS mode, 20 kV, 600 pA, 300 nm beam diameter). H_2O and CO_2 were analysed by gas chromatography of products of ignition at 1200 °C in oxygen atmosphere, using Vario Micro cubeanalyser (Elementar GmBH, Germany).

To obtain an IR absorption spectrum, siudaite powder was mixed with anhydrous KBr, pelletized, and analyzed using an ALPHA FTIR spectrometer (Bruker Optics) at a resolution of 4 cm^{-1}. 16 scans were collected. The IR spectrum of an analogous pellet of pure KBr was used as a reference.

Gamma-resonance studies of siudaite and holotype georgbarsanovite have been carried out by a commercial Mössbauer spectrometer (MS1104Em) to clarify the valence state of iron ions and their environment. The spectrometer is equipped with a standard radioactive source, ^{57}Co, in a rhodium matrix. The absorption-mode measurements have been performed at room temperature. The sample was crushed in an agate mortar, distributed homogeneously within a punch-holder and packed in the form of a tablet to get optimal conditions for measurements. The spectral fitting of the experimental Mössbauer spectrum was carried out by the method of least squares under the assumption of Lorentz-shaped spectral lines. Isomer shifts have been measured relative to metallic iron. The mathematical analysis has been performed by Mössbauer software SpectRelax Version 2.4 (Matsnev and Rusakov 2014).

Powder X-ray diffraction data were measured at room temperature using a Bruker AXS D8 ADVANCE diffractometer equipped with superfast linear position-sensitive detector (LPSD), model VNTEC-1; counting time was 1 s/step in the LPSD "language", equal to ca. 416 s/step in the scintillation counter "language". No monochromator was used, but the radiation was filtered for the $K\beta$ signals.

Single-crystal X-ray studies of siudaite were carried out at 120 K with a Bruker Smart Apex II diffractometer equipped with a CCD-detector using the ω scanning mode. Raw data were integrated using the program SAINT and then scaled, merged, and corrected for Lorentz-polarization effects using the SADABS package (APEX2 2009). A total of 48,418 reflections within the sphere limited by $\theta = 36.52°$ were measured.

Results

General appearance and physical properties

Siudaite forms equant anhedral grains up to 1.5 cm across (Fig. 2). Its colour is yellow to brownish-yellow, the lustre is vitreous, and the streak is white. Peripheral parts of siudaite grains are cherry-red (Fig. 2) because of partial oxidation of Mn^{2+} to Mn^{3+}, which is typical for Mn-rich eudialyte-group minerals from the Khibiny massif (Feklichev et al. 1965; Kostyleva-Labuntsova et al. 1978, p. 321). In this reference, it is to be noted that Mn^{3+} is a strong chromophore, and even low amounts of Mn^{3+} in a mineral result in its red to purple colour. Some grains of altered siudaite are almost completely red, with relics of yellow siudaite in central parts (Fig. 3). All data given in this paper were obtained for inner yellow parts of siudaite grains.

Siudaite is brittle, with the Mohs' hardness of 4½; cleavage is none observed. The fracture is uneven. Density measured by hydrostatic weighing is 2.96(1) g/cm^3. A density of 2.973 g/cm^3 was calculated using the empirical formula and unit-cell parameters obtained from single-crystal X-ray diffraction data.

Optical properties

Under the microscope, siudaite is nonpleochroic, colourless to pale brown in large grains. It is optically uniaxial, negative, with $\omega = 1.635(1)$ and $\varepsilon = 1.626(1)$ ($\lambda = 589$ nm).

The mineral is non-fluorescent under both long- and short-wave UV radiation.

Infrared absorption spectroscopy

Absorption bands in the IR spectrum of siudaite (Fig. 4) and their assignments are (cm^{-1}; s—strong band, w—weak band, sh—shoulder): 3624w, 3500 (broad), 3260sh (O–H stretching vibrations), 1645 (H–O–H bending vibrations), 1504w, 1424w (stretching vibrations of CO_3^{2-} anions), 1135sh, 1060sh, 1012s, 974s, 930sh (Si–O-stretching vibrations), 742, 710sh, 675sh (mixed vibrations of tetrahedral rings—"ring bands"), 532 ($^{V}Fe^{3+}$–O-stretching vibrations), 476, 455, 490sh, 362 (lattice modes involving predominantly bending vibrations of tetrahedral rings, Mn–O, Fe–O and Zr–O-stretching vibrations, as well as librational vibrations of H_2O molecules). The assignment of the IR bands was made in accordance with Rastsvetaeva et al. (2012).

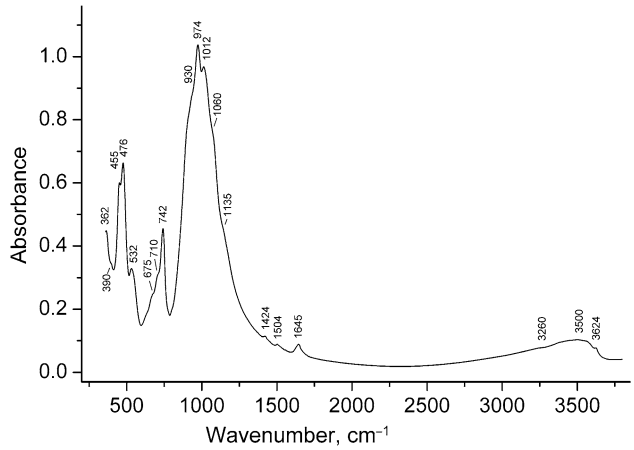

Fig. 4 Powder IR absorption spectrum of siudaite

There are distinct differences between IR spectra of siudaite and those of the chemically related eudialyte-group minerals ikranite and georgbarsanovite (see below). In particular, IR spectrum of georgbarsanovite contains two bands (at 527 and 546 cm^{-1}) corresponding to Fe^{2+}–O-stretching vibrations in *M*2a and *M*2b polyhedra, whereas IR spectrum of ikranite (with Fe^{3+} having predominantly octahedral coordination) does not contain absorption maxima in the range from 525 to 550 cm^{-1} (see supporting information, Fig. 1S). A poor resolution of the bands of Si–O-stretching vibrations in the IR spectrum of ikranite (in the range from 900 to 1100 cm^{-1}) is due to the mixed population of the cation-deficient *M*3 and *M*4 sites.

^{57}Fe Mössbauer spectroscopy

The experimental spectrum of siudaite can be described as a superposition of two symmetric doublets (Fig. 5a). The Mössbauer parameters and assignments of these doublets are listed in Table 1. The strongest (~50%) central quadrupole doublet *a* with IS ~ 0.33 mm/s and QS ~ 0.68 mm/s most likely corresponds to Fe^{3+} at the tetragonal pyramidal *M*2a site. The weak (~23%) *b* doublet with IS ~ 0.35 mm/s and QS ~ 1.11 mm/s can be assigned to Fe^{3+} at the tetragonal pyramidal *M*2b site.

The Mössbauer spectrum of siudaite also contains a broad subspectrum in the form of a large number of quadrupole doublets with different values of the shift and quadrupole splitting. This subspectrum corresponds to Fe^{3+} in an amorphous substance ("zirfesite").

The Mössbauer spectrum of georgbarsanovite, a eudialyte-group mineral chemically related to siudaite, is given

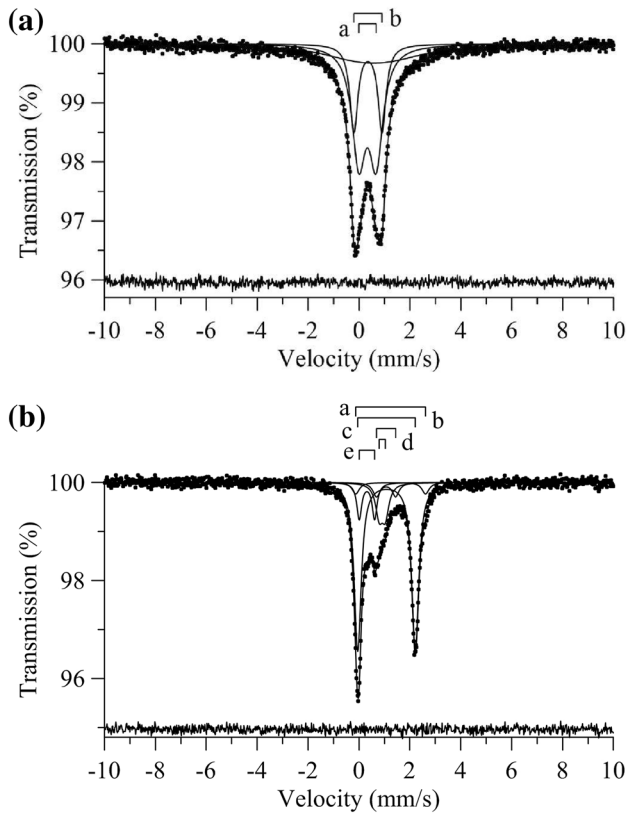

Fig. 5 Mössbauer spectra of **a** siudaite and **b** georgbarsanovite holotype sample

in Fig. 5b for comparison. It is in agreement with the Mössbauer spectrum of georgbarsanovite (sample #3721) published by Khomyakov et al. (2010) and corresponds to the ratio Fe^{2+}: (Fe^{2+} + Fe^{3+}) = 0.704. Three doublets with the relative areas 57.7, 6.4 and 6.3%, isomer shifts 1.086, 1.279 and 0.654 mm/s, and quadrupole splittings 2.263, 2.650, and 1.638 mm/s correspond to Fe^{2+}, and two doublets with the relative areas 15.0 and 14.6%, isomer shifts about 0.65 mm/s, and quadrupole splittings 0.662 and ~ 0 mm/s correspond to Fe^{3+}. Obviously, the strongest doublet with the area of 57.7% refers to Fe^{2+} in the *M*2a site which accumulates 72.9% of total iron (Ekimenkova et al. 2000). Consequently, 14.2% of total iron in georgbarsanovite is Fe^{3+}, which nearly corresponds to the Mössbauer doublet with the relative area of 14.6%. The doublet with the relative area of 15.0% may be assigned to Fe^{2+} in the *M*2b site.

The assignment of the remaining weak doublets (with the areas of 6.4 and 6.3%) in the Mössbauer spectrum of georgbarsanovite is ambiguous. One can suppose that they correspond to Fe^{2+} in the *M*2b site having different environments.

Chemical composition

Analytical data for siudaite are given in Table 2. Contents of other elements with atomic numbers > 8 are below detection limits.

The empirical formula (based on 24.5 Si atoms *pfu*, in accordance with structural data) is $H_{12.11}Na_{8.45}K_{0.41}Ce_{0.31}La_{0.20}Nd_{0.05}Pr_{0.04}Mn_{2.84}Ca_{5.455}Fe^{3+}_{1.76}Ti_{0.21}Zr_{2.95}Hf_{0.04}Nb_{0.65}Si_{24.50}Cl_{0.47}O_{79.12}$. Taking into account structural data, the empirical formula can be rewritten as follows: $[Na_{7.57}(H_2O)_{1.43}]_{\Sigma 9}(Mn_{1.11}Na_{0.88}Ce_{0.31}La_{0.20}Nd_{0.05}Pr_{0.04}K_{0.41})_{\Sigma 3}(H_2O)_{1.8}(Ca_{5.46}Mn_{0.54})_{\Sigma 6}(Fe^{3+}_{1.76}\ Mn^{2+}_{1.19})_{\Sigma 2.95}Nb_{0.65}(Ti_{0.20}Si_{0.50})_{\Sigma 0.71}(Zr_{2.95}Hf_{0.04}Ti_{0.01})_{\Sigma 3}Si_{24.00}Cl_{0.47}O_{70}(OH)_2Cl_{0.47}\cdot 1.82H_2O$.

The simplified formula is $Na_8(Mn^{2+},Na,REE)_3Ca_6(Fe^{3+},Mn^{2+})_3Zr_3(Nb,\square)(Si,\square,Ti)Si_{24}[O_{70}(OH,O)_2](OH,O)_3Cl\cdot 5H_2O$.

The idealized charge-balanced formula is $Na_8(Mn^{2+}{}_2Na)Ca_6Fe^{3+}{}_3Zr_3NbSi_{25}O_{74}(OH)_2Cl\cdot 5H_2O$. It requires Na_2O 8.89, CaO 10.73, MnO 4.52, Fe_2O_3 7.64, ZrO_2 11.78, Nb_2O_5 4.24, SiO_2 47.88, Cl 1.13, H_2O 3.45, −O = Cl −0.26, total 100.00 wt%.

The Gladstone–Dale compatibility index (Mandarino 1981) calculated from the empirical formula and unit-cell parameters found from single-crystal XRD data is 1 − (K_p/K_c) = 0.009 (*superior*).

X-ray diffraction data and crystal structure

Powder X-ray diffraction data for siudaite are listed in Table 3. The trigonal unit-cell parameters refined from the powder data using TOPAS software (Coelho 2007) are: a = 14.1885(26) Å, c = 29.831(7) Å, V = 5200.8(23) Å^3.

Based on the single-crystal X-ray analysis, the following unit-cell parameters have been obtained by the least-squares refinement of all reflections: a = 14.1778(1) Å, c = 29.8071(2) Å, V = 5188.81(4) Å^3. The analysis of

Table 1 Parameters of the Mössbauer spectrum of siudaite at 293 K

Quadrupole doublet	Isomer shift (mm/s)	Quadrupole splitting (mm/s)	Relative area (%)[a]	Assigment
a	0.330(3)	0.681(6)	68.4 ± 1.6	Fe^{3+} in *M*2a
b	0.349(2)	1.105(7)	31.6 ± 1.6	Fe^{3+} in *M*2b

[a]The areas determined after the subtraction of the broad subspectrum corresponding to the admixed amorphous phase ("zirfesite")

Table 2 Chemical composition (in wt%) of siudaite

Constituent	Mean	Range	Standard deviation	Probe standard
Na_2O	8.40	7.82–8.79	0.35	Albite
K_2O	0.62	0.53–0.76	0.09	Orthoclase
CaO	9.81	9.65–10.04	0.12	Wollastonite
La_2O_3	1.03	0.92–1.17	0.08	$LaPO_4$
Ce_2O_3	1.62	1.46–1.85	0.13	$CePO_4$
Pr_2O_3	0.21	0.15–0.30	0.04	$PrPO_4$
Nd_2O_3	0.29	0.21–0.34	0.04	$NdPO_4$
MnO	6.45	6.27–6.76	0.17	MnO_2
Fe_2O_3	4.51	4.34–4.69	0.14	Fe_2O_3
TiO_2	0.54	0.40–0.65	0.09	Ti
ZrO_2	11.67	11.53–11.78	0.10	Zr
HfO_2	0.29	0.25–0.31	0.02	Hf
Nb_2O_5	2.76	2.40–3.23	0.27	Nb
SiO_2	47.20	46.81–47.89	0.43	Albite
Cl	0.54	0.45–0.62	0.06	NaCl
H_2O	3.5 ± 0.2			
CO_2	Bdl			
–O = Cl	–0.12			
Total	99.32			

Despite the content of CO_2 is below detection limit by the CHN analysis, the IR spectrum shows trace amounts of carbonate groups

systematic absences of reflections shows that two space groups are possible, $R\bar{3}m$ and $R3m$, which differ by the presence/absence of the center of the symmetry. Based on the $|E^2\text{-}1|$ statistics we have determined a non-centrosymmetric space group $R3m$, which is common for eudialyte-group minerals.

The structure determination and refinement were carried out using the program packages AREN (Andrianov 1987) and JANA2006 (Petříček et al. 2006). Atomic scattering factors for neutral atoms together with anomalous dispersion corrections were taken from *International Tables for Crystallography* (Prince 2004). Illustrations were produced with the Jana2006 program package in combination with the DIAMOND program (Brandenburg and Putz 2005). The experimental details of the data collection and refinement results are listed in Table 4.

Coordinates of the framework atoms of georgbarsanovite (Ekimenkova et al. 2000) were used as a starting set for the refinement procedure because of its chemical similarity with siudaite. Extra-framework sites including split and partially occupied ones have been localized from the series of difference electron-density maps calculation. Owing to the complex chemical composition, the cation distribution between the structural sites was refined based on crystal-chemical criteria taking into account the atomic displacement parameters, interatomic distances and ionic radii of the cations. The result was controlled by R values and data obtained by means of IR and ^{57}Fe Mössbauer spectroscopy.

The final refinement cycles converged to $R_1 = 3.86$, $wR_2 = 4.21$, and GOF = 1.01 for 2436 independent reflections with $I > 2\sigma(I)$. The highest peak and deepest minimum in the final residual electron-density were 1.67 e Å^{-3} and −0.92 e Å^{-3}, respectively. Table 5 lists the fractional atomic coordinates, occupancy, site symmetry and equivalent atomic displacement parameters (U_{eq}). Selected interatomic distances are given in Table 6.

Siudaite is generally isostructural with other 12-layered members of the eudyalite group with the space group $R3m$ (Fig. 6). Based on the refined site-scattering factors, the crystal-chemical formula of siudaite can be written as follows ($Z = 3$): $\{^{N1-3}[Na_{7.5}(H_2O)_{1.5}]_{\Sigma 9}\ ^{N4}[Mn_{1.11}Na_{0.9}Ce_{0.6}K_{0.39}]_{\Sigma 3}\ ^{N5}[(H_2O)_{1.8}]\}\ ^{M1}[Ca_{5.5}Mn_{0.5}]\ \{[^{M2a}(Fe^{3+}{}_{0.6})^{V}\ ^{M2b}(Fe^{3+}{}_{1.2}Mn_{1.2})^{V}]_{\Sigma 3}\ ^{M3}[Nb_{0.6}]\ ^{M4}[Ti_{0.2}Si_{0.5}]\ (OH,O)_{3.5}\}\ ^{Z}Zr_3\ [Si_3O_9]_2\ [Si_9O_{26}(OH)]_2\ ^{X1}[Cl_{0.47}(H_2O)_{0.42}]\ ^{X2}[(H_2O)_{0.47}]$, where braces and brackets enclose contents of the key sites. Roman numerals denote coordination numbers of atoms.

It is convenient to describe eudialyte-type structures in terms of so-called "key sites", which are considered as species-defining ones (Johnsen et al. 2003; Rastsvetaeva 2007; Rastsvetaeva and Chukanov 2012; Rastsvetaeva et al. 2012). One of them (the $M2$ site) is located at the center of a flat square formed by parallel edges of calcium $M1O_6$-octahedra belonging to adjacent six-membered rings. Due to wide isomorphous substitutions, this site can be shifted from the center of the flat square and complete its coordination to square pyramidal or octahedral by hydroxyl groups and water molecules. In the structure of siudaite, $M2$-site is split into two subsites (Fig. 7), $M2$a and $M2$b, which are located aside the flat square forming $M2a\varphi_5$- and $M2b\varphi_5$-square pyramids ($\varphi = O^{2-}$, OH^-). The distance $M2$a–$M2$b is equal to 0.99 Å. The $M2$a site is occupied by Fe^{3+} (1.2 *apfu*) and Mn (1.2 *apfu*), whereas the $M2$b site is occupied only by Fe^{3+} (0.6 *apfu*). Such distribution of Fe^{3+} within $M2$-sites in the structure of siudaite is confirmed by Mössbauer spectroscopy.

The other key sites, $M3$ and $M4$, (in the case of centrosymmetric space group $R\bar{3}m$ only $M3$-site is present) are located on the threefold axis at the centers of nine-membered Si_9O_{27}-tetrahedral rings. Due to wide heterovalent and heteropolyhedral substitutions in $M3$ and $M4$, these sites are usually split along the threefold axis forming pairs of face shared polyhedra: two tetrahedra ($T + T$), two octahedra ($O + O$) or both tetrahedron and octahedron ($T + O$). These sites can be partially vacant, which increase structural diversity. This feature forms the basis of the modern systematics of eudialyte-group minerals (Rastsvetaeva and Chukanov 2011; Rastsvetaeva et al. 2012). In the structure of siudaite, $M3$-site is occupied by Nb (0.6 *apfu*) in octahedral coordination with the mean distance <Nb–O> = 1.973 Å, while $M4$ is split

Table 3 Powder X-ray diffraction data of siudaite

d_{meas} (Å)	I_{meas} (%)	d_{calc} (Å)[a]	I_{calc} (%)[a]	*hkl*
11.37	18	11.35	23	− 111
9.98	11	9.94	8	800
9.48	11	9.48, 9.48	20, 10	012, 1–12
7.12	42	7.09, 7.09	35, 17	− 120, 110
6.38	60	6.37	33	− 114
6.03	25	6.01, 6.01	5, 3	021, 2–21
5.68	47	5.68	75	− 222
4.98	9	4.97	2	006
4.29	55	4.28	15	− 225
4.11, 4.07	27, 23	4.07, 4.07, 4.07	9, 9, 9	− 126, 116, 2–16
3.946	29	3.939, 3.939, 3.939	14, 7, 14	− 234, 214, 3–14
3.790	29	3.784, 3.784, 3.784	6, 10, 3	033, − 333, 3–33
3.672	9	3.662, 3.662, 3.662	15, 8, 15	− 135, 125, 3–25
3.564, 3.557	17, 27	3.565, 3.565	23, 11	018, 1–18
3.549	32	3.545, 3.545	69, 34	− 240, 220
3.518[b]	17			
3.393, 3.389, 3.341	39, 47, 11	3.383, 3.383, 3.383	35, 35, 35	− 141, 131, 4–31
3.329, 3.324	18, 22	3.320, 3.320, 3.320	10, 10, 10	− 342, 312
3.191	63	3.185	49	− 228
3.165	24	3.159, 3.159, 3.159	19, 13, 10	036, − 336, 3–36
3.145, 3.142	30, 35	3.138, 3.138, 3.138	32, 16, 32	− 237, 217, 3–17
3.015, 3.006	20, 33	3.007, 3.007	30, 15	042, 4–42
2.977, 2.963	25, 100	2.957, 2.957, 2.957	78, 77, 78	− 345, 315, 4–15
2.903	12	2.905, 2.905, 2.905	6, 3, 6	− 138, 128, 3–28
2.891	21	2.885, 2.885, 2.885	21, 21, 21	− 246, 226, 4–26
2.843	99	2.838	100	− 444
2.688	20	2.729, 2.729	3, 2	045, 4–45
2.685, 2.681	21	2.681, 2.681	31, 16	0.2.10, 2.–2.10
2.667, 2.664	15, 15	2.660, 2.660, 2.660	16, 16, 16	− 147, 137, 4–37
2.640	14	2.635, 2.635, 2.635	11, 11, 11	− 354, 324, 5–24
2.581, 2.577	35, 49	2.575, 2.575	42, 21	039, 3–39
2.518	12	2.514, 2.514, 2.514	5, 5, 5	− 348, 318, 4–18
2.512	12	2.508, 2.508, 2.508	6, 3, 6	− 2.3.10, 2.1.10, 3.–1.10
2.453	12	2.447, 2.447	19, 9	051, 5–51
2.373, 2.369	15, 15	2.369, 2.369	22, 11	048, 4–48
2.364	15	2.363, 2.363	11, 6	− 360, 330
2.320, 2.316	9, 11	2.313, 2.313, 2.313	5, 2, 5	− 261, 241, 6–41
2.189	7	2.182, 2.182, 2.182	9, 9, 9	− 162, 152, 6–52
2.164	10	2.162, 2.162, 2.162	3, 1, 3	− 465, 425, 6–25
2.141	15	2.138	18	− 4.4.10
2.119	15	2.120, 2.120, 2.120	7, 7, 7	− 3.4.11, 3.1.11, 4.–1.11
2.051, 2.044	9, 7	2.047, 2.047, 2.047	8, 8, 8	− 3.5.10, 3.2.10, 5.–2.10
2.007	8	2.004, 2.004	4, 2	063, 6–63
1.972	33	1.970, 1.970, 1.970	22, 11, 22	− 468, 428, 6–28
1.924	10	1.924, 1.924, 1.924	7, 7, 7	− 369, 339, 6–39
1.896	11	1.892, 1.892, 1.892	4, 8, 2	066, − 666, 6–66
1.833	15	1.831, 1.831, 1.831	4, 2, 4	− 2.6.10, 2.4.10, 6.–4.10
1.829, 1.827	13, 13	1.828, 1.828, 1.828	11, 5, 11	− 276, − 576, 256
1.777	19	1.773, 1.773, 1.773	3, 3, 3	− 5.6.10, 5.1.10, 6.–1.10
1.775, 1.774	19, 25	1.772, 1.772	43, 22	− 480, 440
1.772	10	1.763, 1.763, 1.763	3, 2, 3	− 4.6.11, 4.2.11, 6.–2.11

Table 3 (continued)

d_{meas} (Å)	I_{meas} (%)	d_{calc} (Å)[a]	I_{calc} (%)[a]	*hkl*
1.753	11	1.751, 1.751, 1.751	5, 5, 5	− 381, 351, 8–51
1.751	10	1.749, 1.749	22, 11	0.4.14, 4.–4.14
1.701	9	1.699, 1.669, 1.669	4, 4, 4	− 2.5.14, 2.3.14, 5.–3.14
1.673	10	1.669, 1.669, 1.669	11, 11, 11	− 486, 446, 8–46
1.639	10	1.637, 1.637, 1.637	5, 5, 5	− 285, 265, 8–65
1.595	10	1.593	16	− 4.4.16
1.591, 1.590	9, 8	1.586, 1.586, 1.586	7, 7, 7	− 1.7.10, 1.6.10, 7.–6.10
1.556	7	1.554, 1.554, 1.554	8, 8, 8	− 3.5.16, 3.2.16, 5.–2.16
1.475, 1.471	8, 9	1.473, 1.473, 1.473	8, 2, 8	− 5.8.11, 0.7.11, 5.3.11

[a]Calculated from single-crystal data

[b]An impurity reflection

into two *M*4a- and *M*4b-subsites (*M*4a–*M*4b = 1.36 Å) statistically occupied by Si (0.5 *apfu*) in the *M*4aφ_4-tetrahedron (< *M*4a–O > = 1.588 Å) and Ti (0.2 *apfu*) in the *M*4bφ_6-octahedron (< M4b–O > = 1.794 Å). Thus, the *M*3 and *M*4 sites contain 40 and 30% vacancies, respectively. Linking of *M*3φ_6- and *M*4bφ_6-octahedra with *M*2φ_5-square pyramids via common OH1 and OH2-vertexes leads to the formation of heteropolyhedral cluster of two types, [Nb(Fe,Mn)$_3\varphi_3$] and [TiFe$_3\varphi_3$], the latter being less occupied than the first one (Fig. 7).

The distribution of large cations over the *N*(1–5) sites in siudaite is also different. The *N*(1–3) sites are predominantly occupied by sodium with admixture of water molecules. Moreover, Na and H_2O-molecules are ordered in the case of the *N*1 and *N*2 sites which is realized in the splitting of the two sites into pairs of subsites with the distances *N*1a–*N*1b = 0.71 Å and *N*2a–*N*2b = 0.99 Å. The *N*1a and *N*2a sites are occupied by sodium (2.4 and 2.55 *apfu*, respectively), while the *N*1b and *N*2b sites are occupied by water molecules (0.6 and 0.45 *apfu*, respectively). *N*3-site is statistically occupied by Na (2.55 *apfu*) and H_2O molecules (0.45 *apfu*).

The *N*4 site is located in the large 9-vertex polyhedron (Fig. 8) and is characterized by a complex chemical composition with the predominance of Mn (1.11 *apfu*) and admixture of Na (0.9 *apfu*), *REE* (0.6 *apfu*), and K (0.39 *apfu*). Due to the statistical occupancy of the split anionic *X*1a and *X*1b sites (by Cl and H_2O, respectively), the mean cation-ligand distances vary from 2.664 Å to 2.697 Å, respectively. Moreover, in the case of the presence of vacancy in the *X*1 site, the coordination of the *N*4 site reduces to a 8-vertex polyhedron with < *N*4–O > = 2.668 Å. Such crystal-chemical features make *N*4-site quite suitable for the occurrence of Mn^{2+}.

The *N*5 site is split into two sites, which are situated in the zeolite-like cavity between adjacent nine-membered Si_9O_{27}-tetrahedral rings and is occupied by water molecules.

Discussion

One of the main features of siudaite is the significant amount of Mn atoms. The presence of trace amount of Mn is detected in most eudialyte-group minerals (Rastsvetaeva et al. 2012). Usually manganese occurs as an impurity element, but in some members of this group its amounts can be up to 3 *apfu* and even more. In most cases, manganese occupies *M*2-site located in the *M*2φ_5-pyramid based on a flat square. Manganoeudialyte is the only manganese-rich mineral of the eudialyte group where Mn completes coordination from 5 to 6 forming *M*2φ_6-octahedron with < Mn–O > = 2.30 Å (Nomura et al. 2010). In calcium-deficient eudialyte-group minerals (with ^{M1}Ca < 4.5 *apfu*), manganese occupies *M*1-site which leads to the ordering of Ca and Mn within the six-membered octahedral ring and lowering of symmetry to *R*3 as it takes place, e.g., in oneillite (Johnsen et al. 1999). The *N*4 site (the most variable among the *N*-sites) in eudialyte-type structures is usually occupied by large cations, different in charge and ionic radii (predominantly Na, but also Sr, K, *REE*). The unique crystal-chemical feature of georgbarsanovite (Khomyakov et al. 2005) is the predominance of Mn in the *N*4-site which is located in the center of the "statistical" 11-vertex polyhedra with the distances varying in the range of 2.484–2.927 Å (mean 2.682 Å). The crystal-chemical role of Mn in eudialyte-type structures has been described in detail by Aksenov et al. (2014).

Siudaite is the second (after georgbarsanovite) member of eudialyte group with the predominance of Mn^{2+} in *N*4-site. In the structure of georgbarsanovite (Ekimenkova et al. 2000), the *N*4 site is occupied predominantly by Mn (1.07 *apfu*) with admixture of Sr, Ce and Ca. Mn is also present in the *N*4 site in the structures of so-called "eucolite" samples (Rastsvetaeva and Borutskii 1990).

Siudaite shows a structural similarity with georgbarsanovite also in the distribution of Fe within the *M*2 site. In georgbarsanovite, the distances in the more occupied *M*2aφ_5-square pyramid are in the range 2.036–2.169

Table 4 Crystal data, data collection information and structure refinement details for siudaite

Crystal data	
Formula	$Na_8(Mn^{2+}{}_2Na)Ca_6Fe^{3+}{}_3Zr_3NbSi_{25}O_{74}(OH)_2Cl{\cdot}5H_2O$
Formula weight (g)	3107.8
Temperature (K)	120
Cell setting	Trigonal
Space group	*R*3*m* (No. 160)
Lattice Parameters	
a (Å)	14.1778(1)
c (Å)	29.8071(2)
V (Å^3)	5188.81(4)
Z	3
Calculated density, D_x (g cm^{-3})	2.983
Crystal size (mm)	0.12 × 0.13 × 0.16
Crystal form	Anhedral grain
Crystal colour	Yellow
Data collection	
Diffractometer	Bruker Smart Apex II (CCD-detector)
Radiation; λ	MoK_α; 0.71073
Absorption coefficient, μ (mm^{-1})	2.946
F (000)	4531
Data range θ (º); *h, k, l*	1.79–36.52; $-23 < h < 23$, $-23 < k < 23$ $-49 < l < 49$
No. of measured reflections	48,418
Total reflections (N_{tot})/unique(N_{ref})	2620/2436
R_{int} (%)	4.89
R_σ (%)	2.21
Criterion for observed reflections	$I > 2\sigma(I)$
Refinement	
Refinement on	Full-matrix least squares on *F*
Weight scheme	$1/(\sigma^2\lvert F\rvert + 0.0016F^2)$
R_1/wR_1	3.86/4.21
R_2/wR_2	4.21/4.90
No. of refinement parameters (N_{par})	263
N_{ref}/N_{par}	9.26
GOF (Goodness of fit)	1.01
Min./max. residual *e* density, (*e* Å^{-3})	– 0.92/1.67

GOF = $\{\sum[w(F_{obs}{}^2 - F_{calc}{}^2)]/(n-p)\}^{1/2}$ where *n* is a number of reflections and *p* is a number of refined parameters

$R_1 = \sum\lvert\lvert F_{obs}\rvert - \lvert F_{calc}\rvert\rvert/\sum\lvert F_{obs}\rvert$; $wR_2 = \{\sum[w(F_{obs}{}^2 - F_{calc}{}^2)^2]/\sum[w(F_{obs}{}^2)^2]\}^{1/2}$

(<*M*2a–O> = 2.109 Å), whereas for the *M*2b site the cation-oxygen distances vary from 1.98 to 2.14 Å (<*M*2b–O> = 2.05 Å). However, the Mössbauer spectroscopy determines the predominant valence state of iron in georgbarsanovite as Fe^{2+} (Khomyakov et al. 2010, this work), whereas in siudaite all iron is Fe^{3+}.

Like georgbarsanovite, siudaite is characterized by the Nb-dominant *M*3 site and the occurrence of Cl and H_2O in the anionic *X* positions on the threefold axis. Siudaite is also chemically related to ikranite $(Na,H_3O)_{15}(Ca,Mn,REE)_6Fe^{3+}{}_2Zr(\square,Zr)(\square,Si)Si_{24}O_{66}(O,OH)_6Cl{\cdot}nH_2O$ (Rastsvetaeva and Chukanov 2003; Chukanov et al. 2003) and, to a less extent, to feklichevite $(Na_{11}Ca_3)Ca_6(Fe^{3+},Fe^{2+})Zr_3NbSi_{25}O_{73}(OH,H_2O,Cl,O)_5$ (Rastsvetaeva et al. 1999; Pekov et al. 2001), and fengchengite $(Na_{12}\square_3)(Ca,Sr)_6Fe^{3+}{}_3Zr_3Si_{24}O_{73}(H_2O,OH)_3(OH,Cl)_2$ (Shen et al. 2011). A distinctive feature of these minerals is the predominance of the Fe^{3+} in *M*2-site. Comparative data for siudaite, georgbarsanovite and ikranite are given in Tables 7 and 8. Ikranite is characterized by a low amount of sodium (Na < 8 *apfu*) which lead to the predominance of vacancies at the *N*3 and *N*5 sites. The *M*3,4-sites in ikranite are also predominantly vacant. A

Table 5 Atom coordinates (*xyz*), site multiplicities (*Q*), equivalent atomic displacement parameters (U_{eq}, Å^2) and site occupancy factors (s.o.f.) in the structure of siudaite

Site	*x*	*y*	*z*	*Q*	$U_{eq/iso*}$	s.o.f.
Z	0.1696(1)	0.3392(1)	−0.1664(1)	9	0.0124(1)	Zr
*M*1	0.0711(1)	0.4065(1)	−0.3341(1)	18	0.0115(2)	$Ca_{0.91}Mn_{0.09}$
Si1	0.2632(1)	0.5264(1)	−0.2528(1)	9	0.0131(4)	Si
Si2	0.0050(1)	0.3971(1)	−0.0972(1)	18	0.0109(3)	Si
Si3	−0.2051(1)	0.2051(1)	−0.0778(1)	9	0.0127(4)	Si
Si4	0.3289(1)	0.2704(1)	−0.2359(1)	18	0.0138(3)	Si
Si5	0.0706(1)	0.1411(1)	−0.0829(1)	9	0.0124(4)	Si
Si6	−0.0833(2)	0.4583(1)	−0.2578(1)	9	0.0182(5)	Si
O1	−0.0293(4)	0.4854(2)	−0.3056(2)	9	0.0188(13)	O
O2	0.2157(2)	0.4314(5)	−0.2895(2)	9	0.0234(14)	O
O3	−0.0625(2)	0.0625(2)	−0.0802(2)	9	0.0211(12)	O
O4	0.0971(2)	0.1942(4)	−0.1322(2)	9	0.0242(14)	O
O5	0.3013(3)	0.2541(3)	−0.2886(1)	18	0.0182(10)	O
O6	−0.0296(4)	0.4852(2)	−0.1144(2)	9	0.0193(13)	O
O7	0.4330(3)	0.3889(3)	−0.2259(2)	18	0.0257(12)	O
O8	−0.2705(2)	0.2705(2)	−0.0806(2)	9	0.0214(13)	$O_{0.6}(OH)_{0.4}$
O9	0.2101(4)	0.6050(2)	−0.2597(2)	9	0.0196(12)	O
O10	0.1082(3)	0.4156(3)	−0.1257(1)	18	0.0218(11)	O
O11	0.3494(5)	0.1747(2)	−0.2164(2)	9	0.0215(15)	O
O12	−0.1814(2)	0.1814(2)	−0.0277(2)	9	0.0162(11)	O
O13	0.0260(3)	0.4119(3)	−0.0438(1)	18	0.0205(11)	O
O14	0.1132(2)	0.2264(4)	−0.0432(2)	9	0.0225(14)	O
O15	−0.0932(3)	0.2736(3)	−0.1075(1)	18	0.0165(9)	O
O16	0.2429(2)	0.4858(4)	−0.2019(2)	9	0.0241(14)	O
O17	0.2286(4)	0.2648(4)	−0.2090(2)	18	0.0294(15)	O
O18	0.7893(5)	0.3946(3)	−0.2592(4)	9	0.058(3)	$O_{0.7}(OH)_{0.3}$
*M*2a	0.2943(1)	0.1471(1)	−0.3364(1)	9	0.0164(3)	$Fe^{3+}{}_{0.40}Mn_{0.40}$
*M*2b	0.3743(6)	0.1871(3)	−0.3326(1)	9	0.023(2)	$Fe^{3+}{}_{0.2}$
*M*3	−0.3333	0.3333	−0.0386(1)	3	0.0111(2)	$Nb_{0.6}$
*M*4a	0.6667	0.3333	−0.2447(3)	3	0.0230(14)	$Si_{0.5}$
*M*4b	0.6667	0.3333	−0.2905(5)	3	0.031(3)	$Ti_{0.2}$
*N*1a	0.1125(3)	0.5563(2)	−0.1802(1)	9	0.0193(10)	$Na_{0.8}$
*N*1b	0.1573(18)	0.5786(9)	−0.1653(7)	9	0.014(3)*	$(H_2O)_{0.2}$
*N*2a	0.2231(2)	0.4463(4)	−0.4871(1)	9	0.0266(12)	$Na_{0.85}$
*N*2b	0.2628(13)	0.526(3)	−0.5093(10)	9	0.020(5)*	$(H_2O)_{0.15}$
*N*3	0.5639(2)	0.1278(4)	−0.3815(1)	9	0.0335(15)	$Na_{0.85}(H_2O)_{0.15}$
*N*4	0.1011(1)	0.2022(1)	−0.2844(1)	9	0.0180(2)	$Mn_{0.37}Na_{0.30}Ce_{0.2}K_{0.13}$
*N*5a	−0.3987(6)	0.2025(12)	−0.1449(5)	9	0.030(4)	$(H_2O)_{0.4}$
*N*5b	−0.3839(15)	0.232(3)	−0.1628(13)	9	0.035(6)*	$(H_2O)_{0.2}$
*X*1a	0	0	−0.2325(3)	3	0.0308(16)	$Cl_{0.47}$
*X*1b	0	0	−0.2558(8)	3	0.019(3)*	$(H_2O)_{0.42}$
*X*2	0.6667	0.3333	−0.4061(11)	3	0.043(6)*	$(H_2O)_{0.47}$
(OH)1	0.1334(5)	0.0667(3)	−0.3359(2)	9	0.0205(15)	$(O,OH)_{0.8}$
(OH)2	0.7277(16)	0.455(3)	−0.3252(12)	9	0.036(6)*	$(OH)_{0.2}$
(OH)3	−0.3333	0.3333	−0.1893(9)	3	0.035(5)	$(OH)_{0.5}$

U_{eq} is defined as one-third of the trace of the orthogonalized U_{ij} tensor

Table 6 Selected interatomic distances (Å) in the structure of siudaite

Zr1	O4	2.052(5)
	O17	2.076(5)×2
	O10	2.086(5)×2
	O16	2.088(5)
		<2.077>
*M*1	O14	2.267(6)
	O2	2.318(5)
	O13	2.354(3)
	O1	2.364(6)
	O5	2.387(3)
	O12	2.397(4)
		<2.348>
Si1	O16	1.597(5)
	O2	1.598(6)
	O9	1.642(6)x2
		<1.620>
Si2	O10	1.596(5)
	O13	1.614(4)
	O15	1.632(3)
	O6	1.636(5)
		<1.620>
Si3	O12	1.601(5)
	O8	1.607(4)
	O15	1.645(4)×2
		<1.625>
Si4	O17	1.598(6)
	O5	1.608(3)
	O7	1.615(3)
	O11	1.631(6)
		<1.613>
Si5	O14	1.580(5)
	O4	1.606(5)
	O3	1.645(4)×2
		<1.619>
Si6	O18	1.564(6)
	O1	1.571(5)
	O7	1.652(5)×2
		<1.610>
*M*2a	(OH)1	1.975(6)
	O13	2.041(5)×2
	O5	2.047(4)×2
		<2.030>
	*M*2b	0.990(8)
*M*2b	O13	1.961(6)×2
	(OH)2	2.108(21)
	O5	2.162(5)×2
		<2.071>
*M*3	(OH)1	1.958(5)×3
	O8	1.988(4)×3
		<1.973>
*M*4a	O18	1.567(5)×3
	(OH)3	1.651(28)
		<1.588>
	*M*4b	1.365(17)
*M*4b	O18	1.771(11)×3
	(OH)2	1.817(41)×3
		<1.794>
*N*1a	O10	2.549(6)×2
	O16	2.585(7)×2
	O6	2.624(6)
	O9	2.656(7)
	O7	2.674(5)×2
		<2.612>
	*N*1b	0.707(22)
*N*1b	O10	2.369(16)×2
	O16	2.448(24)×2
	O6	2.751(22)
	O9	2.887(22)
		<2.545>
*N*2a	O11	2.448(6)
	O3	2.486(7)
	O15	2.601(5)×2
	O4	2.640(8)×2
	O17	2.698(7)×2
		<2.602>
	*N*2b	1.182(35)
*N*2b	*X*1a	2.413(34)
	O4	2.499(34)×2
	O17	2.584(20)×2
	O11	2.832(36)
	O3	2.862(30)
	*X*1b	2.940(38)
		<2.652>
*N*3	O1	2.566(6)
	O13	2.625(5)×2
	*X*2	2.628(10)
	(OH)2	2.763(28)×2
	O10	2.765(5)×2
	O14	2.886(7)
		<2.709>
*N*4	O5	2.554(5)×2
	O12	2.603(4)
	(OH)1	2.671(5)×2
	O17	2.738(6)×2
	O2	2.818(6)
		<2.668>[8]
	*X*1b	2.626(8)
		<2.664>[9]
	*X*1a	2.926(5)
		<2.697>[9]

Table 6 (continued)

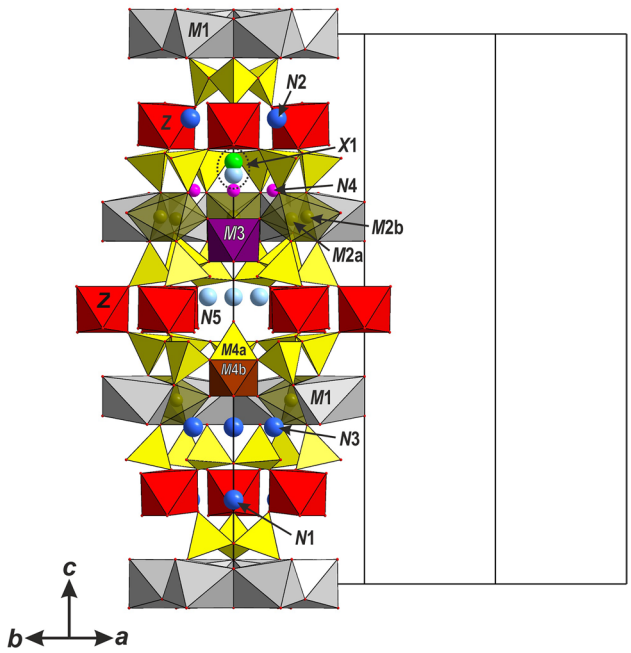

Fig. 6 General view of the siudaite crystal structure. Tridonal unit-cell is outlined by solid line

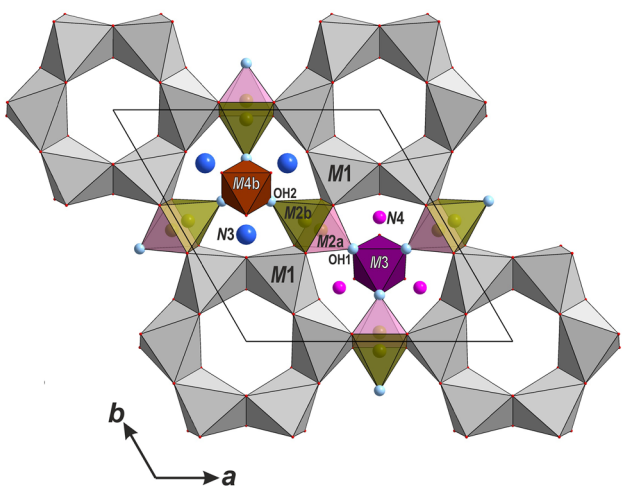

Fig. 7 Distribution of Fe^{3+} over *M*2 sites in the crystal structure of siudaite

high negative charge of the heteropolyhedral framework in the ikranite crystal structure is compensated predominantly by sodium and hydronium H_3O-groups. Fengchengite is also characterized by a low amount of sodium and considerable amount of vacancies at the *N*1-5 and *M*3,4-sites. Sodium deficiency in feklichevite is compensated by calcium, which occupies the *N*4 site (Rastsvetaeva et al. 1999).

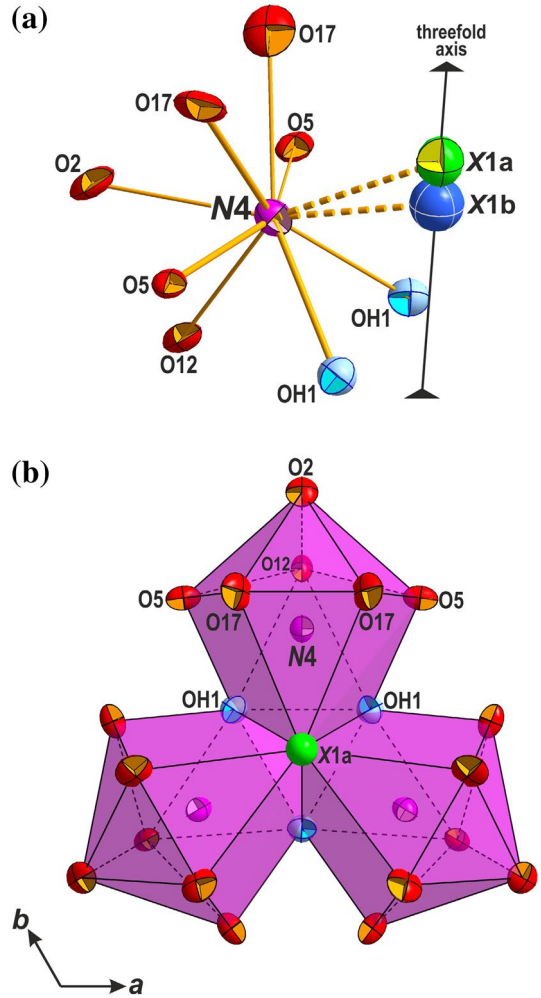

Fig. 8 Coordination of the manganese-dominant *N*4 site (**a**) and linkage of the adjacent *N*4 sites (**b**) in the structure of siudaite

The main distinctive feature of siudaite and georgbarsanovite is high manganese content and simultaneously high iron content. Compositional data on these minerals based on electron microprobe analyses are similar. However siudaite can be distinguished from georgbarsanovite by means of Mössbauer and/or infrared spectroscopic data (by the Fe^{2+}:Fe^{3+} ratio and in the range from 525 to 550 cm^{-1}, respectively). Ikranite differs from siudaite and georgbarsanovite by a lower Mn + Fe content (below 3.5 *apfu* in total) and by the IR spectrum in the ranges 525–550 and 900–1100 cm^{-1}. An indirect diagnostic feature of georgbarsanovite is its greenish colour that is due to the Fe^{2+}–Fe^{3+} charge transfer, whereas unoxidized siudaite and ikranite are yellow to brownish-yellow and become cherry-red to purple as a result of manganese oxidation.

Table 7 Comparison of the occupancies of "key" sites in siudaite and related minerals ($Z=3$)

Site	Siudaite (this work)	Ikranite (Rastsvetaeva and Chukanov 2003)	Georgbarsanovite (Ekimenkova et al. 2000)
*M*1	$^{VI}Ca_6$	$^{VI}[Ca_{4.98}Mn_{0.58}Sr_{0.3}Y_{0.14}]$	$^{VI}Ca_6$
*M*2a	$^{V}[Fe^{3+}{}_{1.2}Mn_{1.2}]$	$^{VI}Fe^{3+}{}_2$	$^{V}[(Fe^{2+},Fe^{3+})_{1.86}Zr_{0.27}Mn_{0.13}Ti_{0.05}]$
*M*2b	$^{V}[Fe^{3+}{}_{0.6}]$		$^{V}Fe^{2+}{}_{0.69}$
*M*3a	$^{VI}Nb_{0.6}$	$^{IV}Si_{0.3}$	$^{VI}Nb_{0.8}{}^{IV}Si_{0.2}$
*M*3b		$^{VI}[Zr_{0.08}Nb_{0.03}Ti_{0.03}]$	
*M*4a	$^{IV}Si_{0.5}{}^{VI}Ti_{0.2}$	$^{VI}[Zr_{0.17}{}^{VI}Nb_{0.07}{}^{VI}Ti_{0.07}]$	^{IV}Si
*M*4b		$^{VI}Zr_{0.15}$	
*N*4	$^{IX}[Mn^{2+}{}_{1.11}Na_{0.9}Ce_{0.6}K_{0.39}]$	$(Na,H_3O)_3$	$^{XI}[Mn^{2+}{}_{1.07}Sr_{0.72}REE_{0.47}Ca_{0.33}K_{0.25}Y_{0.13}Ba_{0.03}]$

Roman numerals indicate coordination numbers of polyhedra

Table 8 Comparative data for siudaite and related eudialyte-group minerals

Mineral	Siudaite	Ikranite	Georgbarsanovite
Formula	$Na_8(Mn^{2+}{}_2Na)Ca_6Fe^{3+}{}_3Zr_3NbSi_{25}O_{74}(OH)_2Cl\cdot5H_2O$	$(Na,H_3O)_{15}(Ca,Mn,REE)_6Fe^{3+}{}_2Zr_3(\square,Zr)(\square,Si)Si_{24}O_{66}(O,OH)_6Cl\cdot nH_2O$	$Na_{12}(Mn^{2+},Sr,REE)_3Ca_6Fe_3{}^{2+}Zr_3NbSi_{25}O_{76}Cl_2\cdot H_2O$
Crystal system	Trigonal	Trigonal	Trigonal
Space group	*R*3*m*	*R*3*m*	*R*3*m*
a, Å	14.1885	14.167	14.262
c, Å	29.831	30.081	29.949
V, Å^3	5200.8	5228.5	5276
Z	3	3	3
Strong lines of the powder X-ray diffraction pattern: *d*, Å (*I*, %)	7.12 (42) 6.38 (60) 4.29 (55) 3.389 (47) 3.191 (63) 2.963 (100) 2.843 (99) 2.577 (49)	6.41 (41) 4.30 (91) 3.521 (57) 3.205 (44) 2.963 (92) 2.841 (100)	6.42 (54) 4.304 (62) 3.202 (100) 3.155 (71) 2.975 (98) 2.857 (94) 2.591 (54)
IR absorption bands	3624w, 3500, 3260sh, 1645, 1504w, 1424w 1135sh, 1060sh, 1012s, 974 s, 930sh, 742, 710sh, 675 s, 532, 476, 455, 490sh, 362	3510, 3280, 1635w, 1000sh, 979 s, 930sh, 743, 700sh, 663, 525sh, 473, 450sh, 420sh	3410w, 1500w, 1465w, 1420w, 1075sh, 1060sh, 1020s, 976 s, 925 s, 740, 704, 690, 657, 610sh, 546, 527, 481, 452
Optical data	Uniaxial (−) $\omega=1.635$ $\varepsilon=1.626$	Uniaxial (+) $\omega=1.612$ $\varepsilon=1.615$	Uniaxial (−) $\omega=1.639$ $\varepsilon=1.631$
Density, g·cm^{-3}	2.96 (meas.) 2.973 (calc.)	2.83 (meas.) 2.83 (calc.)	3.05 (meas.)
Sources	This work	Chukanov et al. (2003), Rastsvetaeva and Chukanov (2003), Chukanov (2014)	Khomyakov et al. (2005), Chukanov (2014)

Acknowledgements This work was financially supported by the Russian Foundation for Basic Research, grants nos. 18-55-18003 (in part of mineralogical and chemical data), 16-05-00739 (in part of single-crystal X-ray analysis) and Russian Science Foundation, Grant No. 14-17-00048 (in part of investigations of physical properties). The authors are grateful to Dr. Axel Sjöqvist and Dr. Jiři Sejlora for valuable comments. The authors thank the Centre for X-ray Diffraction Studies of SPSU and Center for Molecule Composition Studies of INEOS RAS for instrumental support.

References

Ageeva OA, Borutskii BE, Khangulov VV (2002) Eudialyte as a mineralogical and geochemical indicator of metasomatic processes in the formation of poikilitic nepheline syenites of the Khibina Massif. Geochem Int 40(10):997–1003

Aksenov SM, Rastsvetaeva RK, Mitchell RH, Chakrabarty A (2014) Crystal structure of manganese-rich variety of eudialyte from Suchina Hill, India, and manganese ordering in eudialyte-group minerals. Cryst Repts 59(2):146–154

Andrianov VI (1987) Development of the system of crystallographic programs RENTGEN for the computers NORD, CM-4 and EC. Kristallografiya 32:228–231

APEX2 (2009) Bruker AXS Inc., Madison

Brandenburg K, Putz H (2005) DIAMOND Version 3. Crystal Impact GbR. Bonn

Bulakh AG, Petrov TG (2004) Chemical variability of eudialyte group minerals and their sorting. N Jb Miner Mh 3:127–144

Chukanov NV (2014) Infrared spectra of mineral species: extended library. Springer-Verlag GmbH, Dordrecht–Heidelberg–New York–London

Chukanov NV, Pekov IV, Zadov AE, Korovushkin VV, Ekimenkova IA, Rastsvetaeva RK (2003) Ikranite, $(Na,H_3O)_{15}(Ca,Mn,REE)_6Fe^{3+}{}_2Zr_3(\square,Zr)(\square,Si)Si_{24}O_{66}(O,OH)_6Cl\cdot nH_2O$ and raslakite, $Na_{15}Ca_3Fe_3(Na,Zr)_3Zr_3(Si,Nb)(Si_{25}O_{73})(OH,H_2O)_3(Cl,OH)$, the new eudialyte-group minerals from the Lovozero massif. Zapiski Rossiiskogo Mineralogicheskogo Obshchestva (Proc Rus Mineral Soc) 132(5):22–33 (Russian)

Chukanov NV, Pekov IV, Rastsvetaeva RK (2004) Crystal chemistry, properties and synthesis of microporous silicates containing transitional elements. Russ Chem Revs 73(3):227–246

Coelho AA (2007) TOPAS Academic Version 4.1 Technical Reference

Davis P, Stopic S, Balomenos E, Panias D, Paspaliaris I, Friedrich B (2017) Leaching of rare earth elements from eudialyte concentrate by suppressing silica gel formation. Mineral Eng 108:115–122

Ekimenkova IA, Rastsvetaeva RK, Khomyakov AP (2000) Crystal structure of the Fe, Cl-analogue of kentbrooksite. Doklady Chem 370:17–20

Feklichev VG, Razina IS, Kataeva ZT (1965) Eudialyte types of the Khibiny alkaline massif. In: Experimental-methodical investigations of ore minerals. Nauka, Moscow, pp. 188–194 (Russian)

Friedrich B, Hanebuth M, Kruse S, Tremel A, Vossenkaul D (2016) Method for opening a eudialyte mineral. Patent number EP2995692 A1

Johnsen O, Gault RA (1997) Chemical variations in eudialyte. N Jb Miner Abh 171:215–237

Johnsen O, Grice JD (1999) The crystal chemistry of the eudialyte group. Can Mineral 37:865–891

Johnsen O, Grice JD, Gault RA (1999) Oneillite: a new Ca-deficient and *REE*-rich member of the eudialyte group from Mont Saint-Hilaire, Quebec, Canada. Can Mineral 37:1295–1301

Johnsen O, Ferraris G, Gault RA, Grice JD, Kampf AR, Pekov IV (2003) Nomenclature of eudialyte-group minerals. Can Mineral 41:785–794

Khomyakov AP, Nechelyustov GN, Ekimenkova IA, Rastsvetaeva RK (2005) Georgbarsanovite, $Na_{12}(Mn,Sr,REE)_3Ca_6Fe_3{}^{2+}Zr_3NbSi_{25}O_{76}Cl_2\cdot H_2O$, a mineral species of the eudialyte group: revalidation of barsanovite and the new name of the mineral. Zapiski Rossiiskogo Mineralogicheskogo Obshchestva (Proc Rus Mineral Soc) 134(6):47–57 (Russian)

Khomyakov AP, Korovushkin VV, Perfiliev YuD, Cherepanov VM (2010) Location, valence states, and oxidation mechanisms of iron in eudialyte-group minerals from Mössbauer spectroscopy. Phys Chem Miner 37:543–554

Kostyleva-Labuntsova EE, Borutskiy BE, Sokolova MN, Shlyukova ZV, Dorfman MD, Dudkin OB, Kozyreva LV (1978) Mineralogy of the Khibiny Massif. Nauka, Moscow (Russian)

Lebedev VN (2003) Sulfuric acid technology for processing of eudialyte concentrate. Russ J Appl Chem 76(10):1559–1563

Lebedev VN, Shchur TE, Maiorov DV, Popova LA, Serkova RP (2003) Specific features of acid decomposition of eudialyte and certain rare-metal concentrates from Kola Peninsula. Russ J Appl Chem 76(8):1191–1196

Mandarino JA (1981) The Gladstone-Dale relationship: Part IV. The compatibility concept and its application. Can Mineral 19:441–450

Matsnev ME, Rusakov VS (2014) Study of spatial spin-modulated structures by Mössbauer spectroscopy using SpectrRelax. Proceedings of the Conference on Mössbauer Spectroscopy in Materials Science, Hlohovec u Breclavi (Czech Republic), 26–30 May 2014, 40–49. https://doi.org/10.1063/1.4898609

Nomura SF, Atencio D, Chukanov NV, Rastsvetaeva RK, Cutinho JMV, Karipidis TK (2010) Manganoeudialyte, a new mineral from Poços de Caldas, Minas Gerais, Brazil. Zap Ross Mineral Obsh (Proc Rus Mineral Soc) 139(4):35–47

Pekov IV, Ekimenkova IA, Chukanov NV, Rastsvetaeva RK, Kononkova NN, Pekova NA, Zadov AE (2001) Feklichevite $Na_{11}Ca_9(Fe^{3+},Fe^{2+})_2Zr_3Nb[Si_{25}O_{73}](OH,H_2O,Cl,O)_5$, a new mineral of the eudialyte group from Kovdor massif, Kola peninsula. Zap Ross Mineral Obshchestva (Proc Rus Mineral Soc) 130(3):55–65 **(Russian)**

Petříček V, Dušek M, Palatinus L (2006) Structure determination software programs. Institute of Physics, Praha, Czech Republic

Prince E (ed) (2004) International tables for crystallography, volume c: mathematical, physical and chemical tables, 3rd edn. Kluwer Academic Publishers, Dordrecht

Rastsvetaeva RK (2007) Structural mineralogy of eudialyte group: a review. Cryst Repts 52(1):47–64

Rastsvetaeva RK, Borutskii BE (1990) Structural features of *TR*-Fe and *TR*-Mn eucolites. Mineral Zhurnal 12(4):81–88 **(Russian)**

Rastsvetaeva RK, Chukanov NV (2003) Ikranite: composition and structure of a new mineral of the eudialyte group. Cryst Repts 48(5):717–720

Rastsvetaeva RK, Chukanov NV (2012) Classification of eudialyte-group minerals. Geol Ore Deposits 54(7):487–497

Rastsvetaeva RK, Khomyakov AP (2003) Crystal chemistry of modular eudialytes. Cryst Repts 48(Suppl):S69–S81

Rastsvetaeva RK, Ekimenkova IA, Pekov IV (1999) Crystal structure of a new Ca-rich analogue of eudialyte. Dokl Akad Nauk 368(5):636–638 **(Russian)**

Rastsvetaeva RK, Chukanov NV, Aksenov SM (2012) Eudialyte-Group Minerals: Crystal Chemistry, Properties, Genesis. University of Nizhny Novgorod **(in Russian)**

Rastsvetaeva RK, Aksenov SM, Rozenberg KA (2015) Crystal structure of the hydrated analogue of rastsvetaevite. Cryst Repts 60(6):831–840

Schilling J, Marks MAW, Wenzel T, Markl G (2009) Reconstruction of magmatic to subsolidus processes in an agpaitic system using eudialyte textures and composition: a case study from Tamazeght, Morocco. Can Miner 47(2):351–365

Schilling J, Wu F-Y, McCammon C, Wenzel T, Marks MAW, Pfaff K, Jacob DE, Markl G (2011) The compositional variability of eudialyte-group minerals. Mineral Mag 75(1):87–115

Shen G, Xu J, Yao P, Li G (2011) Fengchengite, IMA 2007-018a. CNMNC Newsletter No. 11, December 2011, page 2893. Mineral Mag 75:2887–2893

Sjöqvist ASL, Cornell DH, Andersen T, Erambert M, Ek M, Leijd M (2013) Three compositional varieties of rare-earth element ore: eudialyte-group minerals from the Norra Kärr alkaline complex, Southern Sweden. Minerals 3(1):94–120

Zakharov VI, Maiorov DV, Alishkin AR, Matveev VA (2011) Causes of insufficient recovery of zirconium during acidic processing of Lovozero eudialyte concentrate. Russ J Non-Ferr Met 52(5):423–428